Carbohydrate Polymers 88 (2012) 663–669

Contents lists available at SciVerse ScienceDirect

Carbohydrate Polymers

journal homepage: www.elsevier.com/locate/carbpol

Disulfide cross-linked nanospheres from sodium alginate derivative for inflammatory bowel disease: Preparation, characterization, and in vitro drug release behavior

Dan Chang, Jing Lei, Huiran Cui, Na Lu, Yanjuan Sun, Xiaohua Zhang, Cheng Gao, Hua Zheng[1], Yihua Yin*

Department of Pharmaceutical Engineering, School of Chemical Engineering, Wuhan University of Technology, Wuhan 430070, PR China

ARTICLE INFO

Article history:
Received 31 July 2011
Received in revised form 4 January 2012
Accepted 5 January 2012
Available online 13 January 2012

Keywords:
Sodium alginate derivative
Disulfide cross-linked nanospheres
pH-sensitivity
Reduction-response
Colon-specific drug delivery

ABSTRACT

Reducible sodium alginate nanospheres cross-linked with disulfide linkages were developed for site-specific drug delivery in inflammatory bowel disease. The nanospheres were synthesized by self-assembly of amphiphilic thiolated sodium alginate (TSA) in deionized water and subsequently producing disulfide bond cross-linking. TEM showed that the nanospheres had a spherical core–shell configuration with a size of about 170 nm. Dynamic light scattering showed that the nanospheres had high stability, narrow size distribution and a pH-dependent swelling transition. Cytotoxicity study indicated that the nanospheres had no apparent cell inhibition. Moreover, the size of the nanospheres increased because of the cleavage of disulfides within their network structures in 10 mM glutathione (GSH) solution. As compared with that in GSH-free buffer, the drug release in pH 6.0 buffer with GSH from drug-loaded nanospheres exhibited a marked increase, indicating that the nanospheres may be used for colon-specific drug delivery.

1. Introduction

Inflammatory bowel disease (IBD) is an idiopathic inflammatory disorder involving the mucosa and sub-mucosa of the colon (Makhlof, Tozuka, & Takeuchi, 2009). The conventional treatment of IBD requires frequent drug intake at high doses by oral route, which often leads to absorption in the small intestine and possible strong adverse effects. For example, 5-aminosalicylic acid (5-ASA) is very effective in IBD, but it is absorbed so quickly in the upper gastrointestinal tract (GIT) that it usually fails to reach the colon and leads to significant adverse effects (Nagpal, Singh, Gairola, Bodhankar, & Dhaneshwar, 2006). Oral colon-specific drug delivery system (OCSDDS) brings potential solutions to the problem, because this system can target drugs specifically to the colon and avoid drug release and absorption in the stomach as well as the small intestine, thus reducing drug dosage and side effects.

It is convenient to categorize OCSDDS into four categories (Yang, Chu, & Fix, 2002): time-dependent, pH-dependent, enzyme-dependent and pressure-dependent. Although these approaches may transport anti-inflammatory drugs in adequate concentration and without significant loss before reaching the proximal part of the colon, the lack of selectivity to the colonic lesion area makes them difficult to avoid adverse effects. Hence, a carrier system that delivers the drug specifically to the inflamed tissues would be more desirable.

Recently, a new therapeutic approach targeting the immune regulating cells in IBD using micro/nanoparticulate drug delivery system has been proposed by Nakase et al. (2000). It has been shown that small size particulate drug delivery systems can be efficiently taken up by macrophages and M cells available at the site of inflammation. Moreover, the disruption of the intestinal barrier function could allow for the accumulation of the particulate delivery system at the site of inflammation (Stein, Ries, & Barret, 1998). Lamprecht, Schafer, and Lehr (2001) have observed that this accumulation is particle-size-dependent. When the particle size decreases, the accumulation effect will increase and reach maximum at around 100 nm. Furthermore, Dahan, Amidon, and Zimmermann (2010) have reported that particles with negative surface charges can adhere to inflamed tissue more easily, due to the high concentration of the proteins with positive charges in inflamed tissue. Based on these considerations, drugs encapsulated in nanoparticles with negative surface charges are more likely to enrich in the site of inflammation.

As intracellular controlled release carriers, polymers containing disulfide-bonds and their self-assembly have been investigated widely in recent years. The disulfide-bonds in these polymers can be formed spontaneously by autoxidation of thiols, primarily via oxidation upon exposure to air. They have excellent

* Corresponding author. Tel.: +86 027 87859019; fax: +86 027 87859019.
E-mail address: yihuayin@yahoo.com.cn (Y. Yin).
[1] Co-corresponding author.

0144-8617/$ – see front matter © 2012 Elsevier Ltd. All rights reserved.
doi:10.1016/j.carbpol.2012.01.020

stability in extracellular fluids, whereas can reversibly be cleaved in an intracellular reductive environment such as GSH (2–10 mM) (Arrick & Nathan, 1984), and trigger drug release from the carriers. Oral colon-specific drug delivery system must pass through the stomach and small intestine, and the fraction of anaerobes increases from proximal small bowel to distal, reaching 99% of bacterial species in the colon (Hooper et al., 2001). The distribution causes changes in redox potential along the GIT, which are the expression of total metabolic and enzyme activity. The redox potential of the proximal small bowel has been found to be -67 ± 90 mV; it is -196 ± 97 mV in the distal small bowel and -415 ± 72 mV in the right colon (Stirrup et al., 1990; Wilding, Davis, & O'Hagan, 1994). The redox potential in the colon is a lot lower than the standard reduction potential for disulfide bonds (about −250 mV), thus reductive cleavage of disulfide bonds is likely.

Alginate is a natural anionic polyelectrolyte consisting of linear of α-L-guluronic acid and β-D-mannuronic acid with properties such as a high degree of aqueous solubility, a high tendency for gelation in proper condition, biocompatibility, and non-toxicity (Hamidi, Azadi, & Rafiei, 2008). Alginate nanoparticles can be easily obtained by calcium-induced gelation or by the addition of an aqueous polycationic polymer to form a polyelectrolyte complex (Sundar, Kundu, & Kundu, 2011). However, the nanoparticles prepared via calcium-induced gelation are physically cross-linked, and their structures are unstable in high pH media and the drug release behaviors are also not easily controlled (George & Abraham, 2006). The stabilities of the nanoparticles obtained by complex interactions are also dependent on pH. For example, the diameter of polyelectrolyte complex nanoparticles based on alginate and chitosan significantly increases as the pH increases between 6.4 and 6.7. The observed particle diameter at pH 7.0 is about 50 times the size observed at pH 6.0 (Sather, Holme, Maurstad, Smidsrød, & Stokke, 2008). Since the pH of the small intestine is between 6 and 8, it is difficult to control drugs to colon using the complex nanoparticles as OCSDDS.

In this work, a kind of novel pH-sensitive and reduction-responsive nanospheres for site-specific drug delivery to the inflamed colonic tissues was prepared. Sodium alginate (SA) was first oxidized with sodium periodate, and then modified by immobilization of a hydrophobic thiol-bearing ligand, namely 4-aminothiophenol (4-ATP), to the backbone of SA. This modified derivative could form core cross-linked nanospheres by self-assembly in deionized water and subsequently the air oxidation of thiol groups to disulfide bonds. The cross-linked nanospheres were characterized by dynamic light scattering (DLS) and transmission electron microscope (TEM). The pH-sensitivity, reduction-response and cell cytotoxicity were investigated, and the in vitro drug release from the 5-ASA-loaded nanospheres was also studied in simulated gastrointestinal media.

2. Materials and methods

2.1. Materials

Sodium alginate (the viscosity of 2% solution is 3200 mPa s at 25 °C) was obtained from Enterprise Group Chemical Reagent Co. Ltd. 4-ATP and 5-aminosalicylic acid (5-ASA) were purchased from Sigma Chemical Co. 5,5′-Dithiobis (2-nitrobenzoic acid) (DTNB) and GSH were purchased from Biosharp. Dulbecco's modified Eagle's medium (DMEM) was obtained from Gibco. 3-(4,5-dimethylthiazol-2-yl)-2,5-diphenyltetrazolium bromide (MTT) was from Amresco. All other chemicals were of analytical grade.

2.2. Synthesis of partially oxidized sodium alginate

Partially oxidized sodium alginate (OSA) was prepared according to a previously reported method (Gomez, Rinaudo, & Villar, 2007). The oxidation reaction was carried out at room temperature during 24 h. In a dark bottle, SA was diluted to 1% in deionized water and then sodium periodate aqueous solution was added under stirring. The ratios between repetitive unit and sodium periodate were 10:1, 10:3 and 10:5. 5 mL of ethylene glycol was added after 24 h to stop the reaction. The resultant solution was filtered, washed with ethanol and dried under vacuum at room temperature. The degree of oxidation (DO, %) was determined by the hydroxylamine hydrochloride method (Zhao & Heindel, 1991). In the feed molar ratios of 10:1, 10:3 and 10:5 between repetitive unit of SA and sodium periodate, three samples were synthesized. Their degrees of oxidation (%) were 9.48, 27.83, and 44.36.

2.3. Synthesis and characterization of TSA

0.05 g of OSA (DO% = 44.36) prepared above was solubilized in 6 mL of deionized water, and then 4 mL of ethanol was added dropwise with stirring. After the mixture was mixed evenly, 4-ATP dissolved in 2 mL of ethanol was added dropwise into the OSA solution. The reaction mixture was stirred at room temperature. After 6 h, 0.1 g of sodium borohydride was added and the pH was adjusted to 7.0 with 0.1 M HCl in order to reduce disulfide bonds and Schiff bases. The reaction mixture was stirred for another hour under nitrogen at 4 °C. The solution was dialyzed under nitrogen atmosphere to minimize oxidation of thiol groups, and then lyophilized. The light yellow product was characterized by FT-IR spectroscopy, UV–vis spectroscopy and ^{1}H NMR spectroscopy. The content of free thiol groups on the product was determined with Ellman's method (Bernkop, Hornof, & Zoidl, 2003). In the feed molar ratios of 1:0.5, 1:1 and 1:1.5 between aldehyde group of OSA and amino group of 4-ATP, three samples were synthesized and named as TSA-1, TSA-2 and TSA-3, respectively. Their contents of free thiol groups (μmol SH/g polymer) were 191.8, 298.9, and 441.8.

2.4. Preparation and characterization of disulfide cross-linked nanospheres

0.05 g of TSA was dissolved in 20 mL of deionized water and stirred for 1 h at 4 °C. Then the solution was incubated for 24 h away from light at room temperature. Afterwards, the solution was ultrasonicated for 3 min using an ultrasonic cell shredder JY-92 IIDN (40 W) to facilitate the oxidation reaction of thiol groups. The nanosphere sample prepared using TSA-1, TSA-2 and TSA-3 was named as NS-1, NS-2 and NS-3, respectively. The thiol groups on the nanospheres were measured with Ellman's reagent. The hydrodynamic mean diameter (MD), the size distribution and the ζ potential of the nanospheres were determined by DLS using a Zetasizer 4 (Malvern Instruments, Herrenberg, Germany). Scattering light was detected at 90° angle at a temperature of 25 °C. Samples were diluted with filtered (0.45 μm pore size) deionized water before measurements to obtain a count rate in the appropriate range. Morphological evaluation of the nanospheres was performed by TEM using a JEM-100CX11 (JEOL, Japan).

2.5. Stability studies of disulfide cross-linked nanospheres

The stability of the disulfide cross-linked nanospheres was investigated by DLS. The nanospheres were placed at room temperature for a month in buffer solution of pH 7.4, and then the particle sizes and distributions were measured.

2.6. pH-sensitivity studies of disulfide cross-linked nanospheres

A certain volume of nanosphere suspension was divided into seven parts and then the pH value of each part was adjusted with 0.1 M HCl and 0.1 M NaOH. To keep the ionic strengths of the media constant at 0.1 M, sodium chloride was added. Then, the pH-sensitivities of the disulfide cross-linked nanospheres were studied by measurements of the mean particle diameter within aqueous media at 25 °C.

2.7. Reduction-response studies of disulfide cross-linked nanospheres

The reduction-response of disulfide cross-linked nanospheres was studied at 25 °C in buffer solution of pH 7.4 using DLS. The NS-3 suspension was divided into three parts. One part was used as a control; the other two parts were used for reduction-response studies by adding GSH to reach the final concentrations of 10 μM and 10 mM, respectively. After the three samples were placed for a day, the particle sizes and distributions of the nanospheres were obtained by DLS. The particle size of the sample placed for 7 days in pH 7.4 buffer containing 10 mM GSH was also measured.

2.8. Cytotoxicity assay

Caco-2 cells used for MTT assay were seeded on 24-well culture plates at a density of 1×10^4 cells per well in DMEM culture medium. The cells were grown in an atmosphere of 95% air, 5% CO_2 at 37 °C and 90% humidity for 24 h. After attachment of Caco-2 cells to the plates, they were incubated with 200 μL DMEM containing the cross-linked nanospheres or unmodified SA with the concentration of 0.5% (w/v), and then the mixtures were placed in an incubator for 48 h. Subsequently, the culture medium was replaced by fresh DMEM and 30 μL MTT solution with the concentration of 0.5 mg/L was added to the Caco-2 cells. After incubation for 4 h, 200 μL DMSO was added and the mixtures were shaken at 37 °C. The optical densities (OD) were measured at 570 nm with a microplate reader (Bio-Rad 550). The cell viability was calculated as follows:

$$\text{Cell viability}(\%) = \left(\frac{\text{OD}_{\text{treated}}}{\text{OD}_{\text{control}}}\right) \times 100 \quad (1)$$

where $\text{OD}_{\text{control}}$ was obtained without the cross-linked nanospheres or unmodified SA and $\text{OD}_{\text{treated}}$ was obtained in the presence of the nanospheres or unmodified SA.

2.9. Preparation of drug-loaded nanospheres

0.1 g of TSA was dissolved in 100 mL of deionized water under stirring, and then 0.003 M of 5-ASA was added to the solution and continuously stirred for 1 h at 4 °C. After being incubated for 24 h away from light at room temperature, the solution was ultrasonicated for 3 min to obtain drug-loaded nanosphere solution.

For the determination of drug-loading efficiency, the drug-loaded nanospheres were collected by high-speed centrifugation at 8000 rpm for 15 min, washed three times with a little bit of deionized water to remove the free drug, and then freeze-dried to obtain drug-loaded nanospheres. The concentrations of 5-ASA in the decanted aqueous solution and the three washing solutions were determined by measuring the absorbance at 330 nm using a UV1700PC-UV-Visible Spectrophotometer (Phenix, China). The determinations were made in triplicate, and the results were averaged. Drug-loading efficiency was determined as follows:

$$\text{Drug-loading efficiency}(\%) = \left(\frac{W}{W_0}\right) \times 100 \quad (2)$$

where W is the mass of drug in nanospheres and W_0 is the mass of drug-loaded nanospheres.

The drug-loading efficiency (%) of NS-1, NS-2, and NS-3 was 3.65, 5.16 and 4.73, respectively.

2.10. In vitro release studies

The in vitro release behaviors of 5-ASA from the cross-linked nanospheres were studied at 37 ± 0.1 °C in a thermostatic rotary shaker at shaking speed of 50 rpm. The simulated gastrointestinal media used for the release of 5-ASA were 30 mL of pH 1.0 hydrochloric acid solution (simulating the pH in the stomach), pH 7.4 phosphate buffer solution (simulating the pH in the small intestine), pH 6.0 phosphate buffer solution (simulating the pH in the colon), and pH 6.0 phosphate buffer solution with 25 mM GSH (simulating the pH and reductive medium in the colon). Two drug-loaded samples (30 mg) were respectively suspended in a pH 1.0 hydrochloric acid solution for 2.0 h. Then the nanospheres were collected by ultracentrifugation and again placed into a pH 7.4 phosphate buffer for 3.0 h. Subsequently, the nanospheres were isolated by ultracentrifugation once again. One sample was put into a pH 6.0 phosphate buffer as a control and the other was put into a pH 6.0 phosphate buffer containing GSH. At predetermined time intervals, 5 mL portions of the two release media were withdrawn and replenished with equal volume of fresh media. The concentrations of 5-ASA were determined with UV-Visible Spectrophotometer at 330 nm. The cumulative drug release was calculated as follows:

$$\text{Cumulative drug release}(\%) = \left(\frac{M_t}{M_0}\right) \times 100 \quad (3)$$

where M_t is the amount of drug released at time t and M_0 is the initial amount of drug in nanospheres. The release data were averaged based on three independent measurements.

3. Results and discussion

3.1. Synthesis and characterization of TSA

TSA was synthesized according to the procedure as shown in Fig. 1(A). During the process, SA was oxidated with sodium periodate to obtain OSA. Subsequently, the aldehyde groups of OSA reacted with the amino groups of 4-ATP to form Schiff bases. Finally, sodium borohydride was used for reductive amination to afford TSA. The structures of OSA and TSA were characterized by FT-IR spectrum and ^{1}H NMR spectroscopy.

The FT-IR spectra of SA (see curve a), OSA (see curve b) and TSA (see curve c) are shown in Fig. 2. Compared with curve a, curve b presented a new characteristic band at 1727 cm^{-1} (as shown in Fig. 2(b)), which was assigned to aldehyde group (C=O). The other two characteristic bands of C (O)—H of aldehyde groups should be at 2820 cm^{-1} and 2720 cm^{-1}, which were covered by C—H alkyl absorption band. Compared with curve b, a new characteristic band at 2540 cm^{-1} was observed in TSA spectrum (as shown in Fig. 2(c)), which indicated the existence of thiol groups. A new characteristic band at 1494 cm^{-1} was assigned to a stretching vibration of benzene ring, and another obvious characteristic absorption band of the benzene ring should be at 1600 cm^{-1}, which was covered by carbonyl group absorption band. A new characteristic band at 1436 cm^{-1} was assigned to C—N stretching vibration. These results indicated that 4-ATP was linked on OSA.

The chemical structures of SA (see curve a), OSA (see curve b) and TSA (see curve c) were determined by ^{1}H NMR spectroscopy. The presence of peak at δ 8.4 in the ^{1}H NMR spectrum (as shown in Fig. 3(A (b))) corresponded to the proton of aldehyde group, which indicated the formation of aldehyde groups in the OSA structure. The peaks at δ 6.8 and δ 7.4 were attributed to benzene ring of

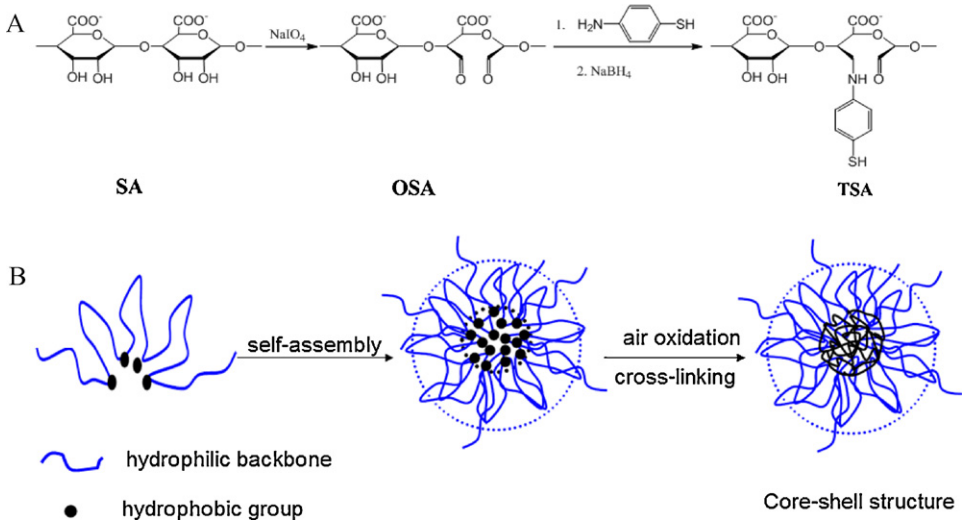

Fig. 1. (A) Synthetic scheme of TSA and (B) assembly process of disulfide cross-linked nanospheres.

4-ATP and the peak at δ 1.8 corresponded to the proton of thiol group (see Fig. 3(A)). UV–vis spectroscopy further supported the above-mentioned points. Compared with that in the curve of OSA, a strong UV absorption peak at 256 nm in the curve of TSA was observed, which suggested that a new substance was formed, and the peak may be attributed to the conjugation of benzene ring (see Fig. 3 (B)).

3.2. Preparation and characterization of disulfide cross-linked nanospheres

Disulfide cross-linked nanospheres were synthesized according to the procedure as shown in Fig. 1(B). A certain amount of TSA was first dissolved in deionized water. During this process, TSA formed disulfide cross-linked core–shell particles via self-assembly and subsequent air oxidation. The TEM photograph in an aqueous medium at pH 7.0 was shown in Fig. 4(A). The nanospheres had a spherical core–shell configuration and a relatively uniform size, and their mean size was about 170 nm. The remaining thiol groups on the cross-linked nanospheres were determined by Ellman's method to be less than 10% of the initial value, and this indicated that thiols were oxidized to form disulfide bonds.

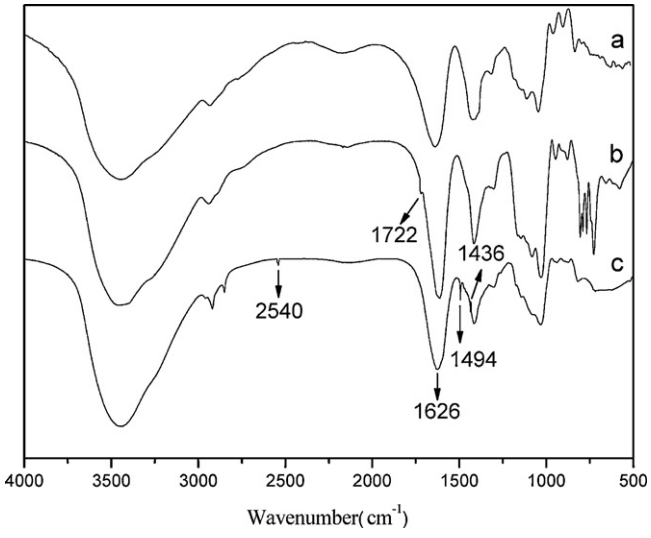

Fig. 2. FT-IR spectra of: SA (a), OSA (b) and TSA (c).

On the basis of the amount of free thiol groups in the resulting TSA determined with Ellman's reagent, the molar ratio between ATP and glycosyl in the aggregates could be calculated. For nanospheres, the ratio was about 1/16.7, which meant there existed few units grafted with ATP and longer hydrophilic chain segments in TSA chains. The hydrophilic chain segments without ATP had the stronger electrostatic repulsion between the $-COO^-$ groups and a higher affinity with water molecules, and tended to the more extend in aqueous solution. To counteract the hydrophilic interaction, the stronger hydrophobic interaction offered by more hydrophobic groups was necessary. As a result, a hydrophobic core was formed by ATP groups from more TSA chains and the longer hydrophilic segments in the chains coiled to build a shell outside the hydrophobic core. Furthermore, inter- and/or intra-molecular hydrogen bonds among tightly packed TSA backbones also promoted the self-aggregation of TSA molecules. Subsequently, the nanoparticle solution was ultrasonically treated to facilitate the formation of disulfide linkages between adjacent thiol groups via air oxidation, and core cross-linked nanospheres were obtained.

3.3. Stability studies of disulfide cross-linked nanospheres

Table 1 shows the particle sizes and distributions of nanospheres before and after being placed for a month. It can directly be seen that the nanospheres had little size change and small polydispersity index (PDI) values. These results suggested that the disulfide cross-linked nanospheres had high stability. This may be attributed to the formation of inter- and intra-molecular disulfide bonds. This kind of stability is of great significance for avoiding drug release before nanospheres reaching targeted location. The ζ potentials of nanospheres are also shown in Table 1. It demonstrated that the nanospheres had negative surface charges. In view of report in the literature that particles with negative surface charges adhere to inflamed tissue more easily, so the nanospheres prepared in this study are beneficial for delivering a drug specifically to the inflamed sites.

3.4. pH-sensitivity studies of disulfide cross-linked nanospheres

The pH-sensitivity of disulfide cross-linked nanospheres was studied by measurements of the mean particle diameters within aqueous media of different pH values. As shown in Fig. 4(B), the diameters of all samples increased with increasing pH value, and the extent of the change was decreased in the following order:

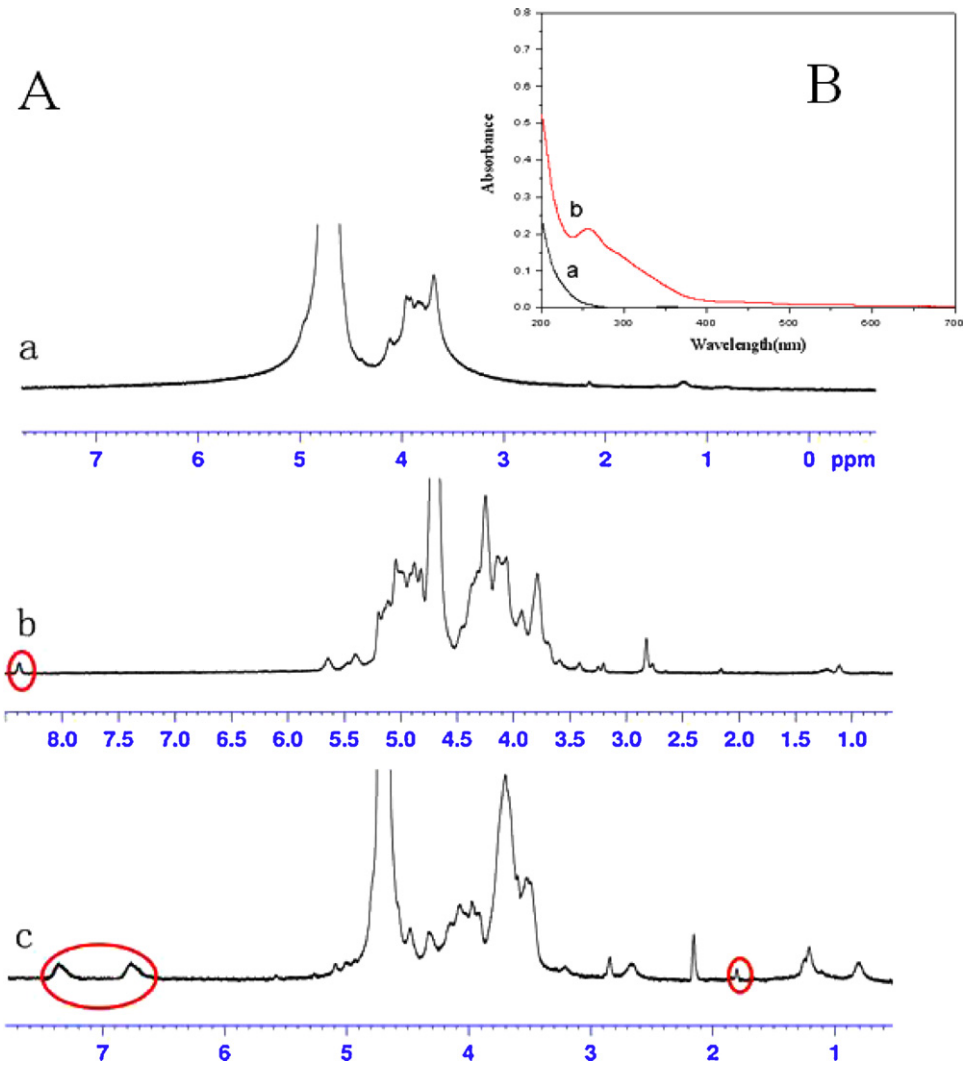

Fig. 3. (A) ^{1}H NMR spectra in D_2O of: SA (a), OSA (b) and TSA (c); (B) UV–vis spectra of OSA (a) and TSA (b).

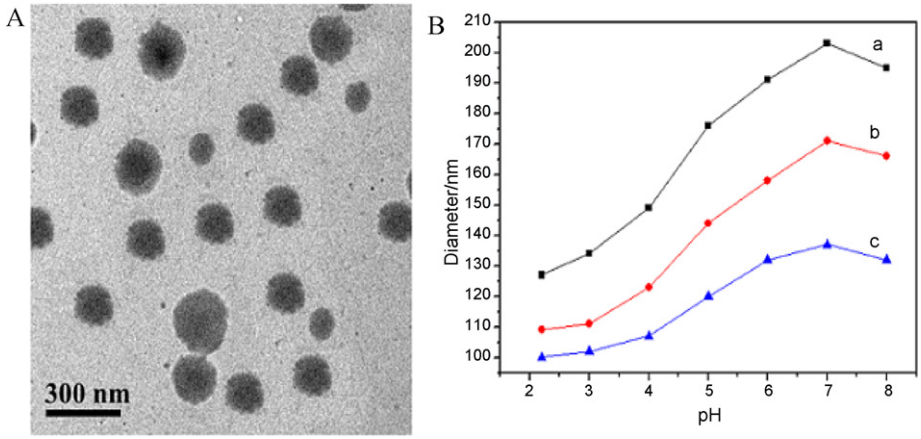

Fig. 4. (A) TEM photograph of the disulfide cross-linked nanospheres (NS-2) in aqueous medium at pH 7.0; (B) pH-sensitivities of NS-1 (a), NS-2 (b) and NS-3 (c).

Table 1
The particle sizes and distributions and ζ potentials of nanospheres at pH 7.4 for their stability.

Sample	Before storage		After storage		ζ potential (mV)
	MD (nm)	PDI	MD (nm)	PDI	
NS-1	203 ± 0.14	0.084 ± 0.017	209 ± 0.18	0.090 ± 0.016	−25.7
NS-2	171 ± 0.15	0.063 ± 0.012	168 ± 0.14	0.062 ± 0.012	−22.2
NS-3	137 ± 0.17	0.071 ± 0.015	140 ± 0.12	0.065 ± 0.018	−20.3

Table 2
The particle sizes and distributions of nanospheres at pH 7.4 containing various concentrations of GSH for 24 h.

Sample	GSH (0)		GSH (10 μM)		GSH (10 mM)	
	MD (nm)	PDI	MD (nm)	PDI	MD (nm)	PDI
NS-1	200 ± 0.15	0.088 ± 0.018	207 ± 0.17	0.091 ± 0.022	278 ± 0.38	0.223 ± 0.038
NS-2	177 ± 0.18	0.060 ± 0.016	180 ± 0.16	0.063 ± 0.019	236 ± 0.32	0.218 ± 0.042
NS-3	140 ± 0.16	0.080 ± 0.008	141 ± 0.17	0.081 ± 0.014	211 ± 0.22	0.215 ± 0.035

NS-1 > NS-2 > NS-3. For each of three samples the particle diameter was smaller at low pH value and had a maximum at pH 7.0. In the range of pH 2–7, the radius of the nanospheres based on NS-1 increased by a factor of about 1.6, while the sample based on NS-3 only increased by about 1.3 and indicated that an increase in the cross-linking degree lead to a low pH-sensitivity. The pH sensitivity of the nanospheres was ascribed to the following reasons. Due to the protonation of carboxyl groups of alginate in pH 2–4 media, a lot of hydrogen bonds in the hydrophilic shells of nanospheres were formed. These hydrogen bonds caused a compact structure, so a smaller particle size was observed. While in pH 5–7 media, the free carboxylic acid groups would be ionized, which would break hydrogen bonds and generated electrostatic repulsion among polymer hydrophilic chain segments. So a larger particle size would be observed. Subsequently, a decreased particle diameter in pH 7–8 may be ascribed to the charge screening effect of the counter ions (Hua & Wang, 2009; Pourjavadi, Sadeghi, & Hosseinzadeh, 2004).

3.5. Reduction-response studies of disulfide cross-linked nanospheres

The particle sizes and distributions of nanoparticles in pH 7.4 buffer solutions with GSH of different concentrations (0, 10 μM and 10 mM) for 24 h are shown in Table 2. The nanospheres were stable in buffer solutions without GSH and with 10 μM GSH, and the particles nearly maintained the same size and PDI value. In the buffer medium containing millimolar GSH, in contrast, the obvious increase in particle size and distribution could be observed. Furthermore, the trend of the increase was more obvious with the extension of time. The particle diameter of NS-3 placed for 7 days (495 ± 24.7 nm) was much larger than that of NS-3 placed for 1 day (140 ± 0.16 nm).

3.6. Assessment of cytotoxicity

The cell viabilities of Caco-2 cells were investigated by measuring OD before and after treatment with 0.5% solutions of the cross-linked nanospheres or unmodified SA. As shown in Fig. 5, Caco-2 cells still had high viabilities after being treated with the cross-linked nanospheres. The observed cell viabilities of cross-linked nanospheres do not differ significantly from SA. The result indicates that the disulfide cross-linked nanospheres have no apparent cytotoxicity in the concentration range we studied.

3.7. In vitro release studies

5-ASA is an anti-inflammatory drug widely used in the treatment of inflammatory bowel disease, and it was chosen as model drug in this study. In vitro release from the disulfide cross-linked 5-ASA-loaded nanospheres was investigated in simulated gastrointestinal conditions. In view of reports in the literature, the redox potential in the colon is about −415 ± 72 mV (Sinha & Kumria, 2003). GSH with a standard potential of −270 mV was utilized as a reducing agent to simulate the reducing environment of the colon (Aslund, Berndt, & Holmgren, 1997). The stomach passage with GSH was not investigated within this study since GSH in the stomach will not cause cleavage of disulfide bonds as its redox activity is too low at pH ≤ 4 (Finley, Wheeler, & Witt, 1981).

Fig. 6(A) shows the percentage of 5-ASA released as a function of time from the disulfide cross-linked drug-loaded NS-2 during simulated gastrointestinal conditions likely to be encountered during intestinal transit to the colon. First, the samples were put in pH 1.0 GSH-free buffer for 2.0 h, then in pH 7.4 GSH-free buffer for 3.0 h, finally in pH 6.0 buffer with GSH for 10 h. The pH 6.0 medium without GSH was used as a control. The release profiles revealed that, there was only about less than 14.8% of 5-ASA released during the first 5.0 h in GSH-free media. The cumulative amount of 5-ASA released over 15 h in the GSH-free media was around 25%. As compared with the control, the release of 5-ASA was increased markedly when the drug-loaded nanospheres were exposed to pH 6.0 medium with GSH, with more than 80% 5-ASA released over 15 h, indicating that disulfide cross-linking bonds in the nanospheres were still available for cleavage by GSH, as a consequence, resulted in enhanced 5-ASA release.

Fig. 6(B) shows the effect of the contents of free thiol groups on the release of the disulfide cross-linked 5-ASA-loaded nanospheres. NS-1, NS-2 and NS-3 had similar release profiles in simulated gastrointestinal media. There was little difference between the drug release in simulated stomach and small intestine media. However, their cumulative amount of 5-ASA released at the same time in simulated colon medium decreased in this order: NS-1 > NS-2 > NS-3. The result may be attributed to an increase in the degree of disulfide cross-linking, which makes it more difficult for 5-ASA to diffuse.

The release mechanism of hydrophilic drug is generally based on the diffusion process by means of water as a medium. When a pH-sensitive core–shell nanosphere is placed in acidic buffer medium, the hydrophilic shell contraction would hinder or restrict the penetration of water inside the nanosphere and resulting in a slow initial release. With the increase of pH, the swelling of hydrophilic shell would enhance the release of drug inside it. 5-ASA is a hydrophilic drug, but it is only very slightly soluble in water. Thus, for a 5-ASA-loaded nanoparticle prepared in water, it can be speculated that 5-ASA may be mainly distributed inside the hydrophobic core of

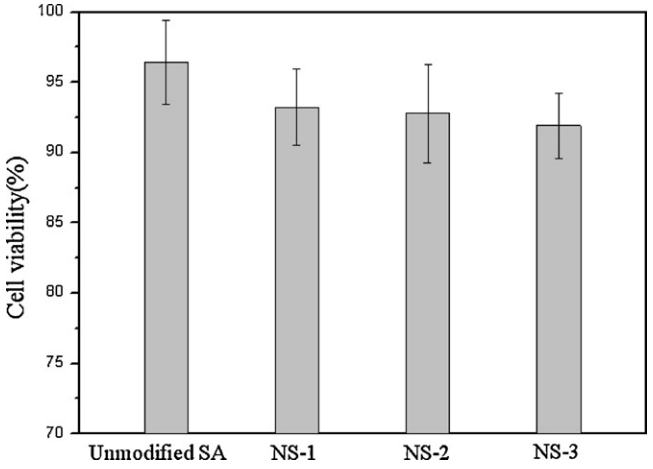

Fig. 5. Cell viability of the disulfide cross-linked nanospheres (NS-1, NS-2 and NS-3) and unmodified SA.

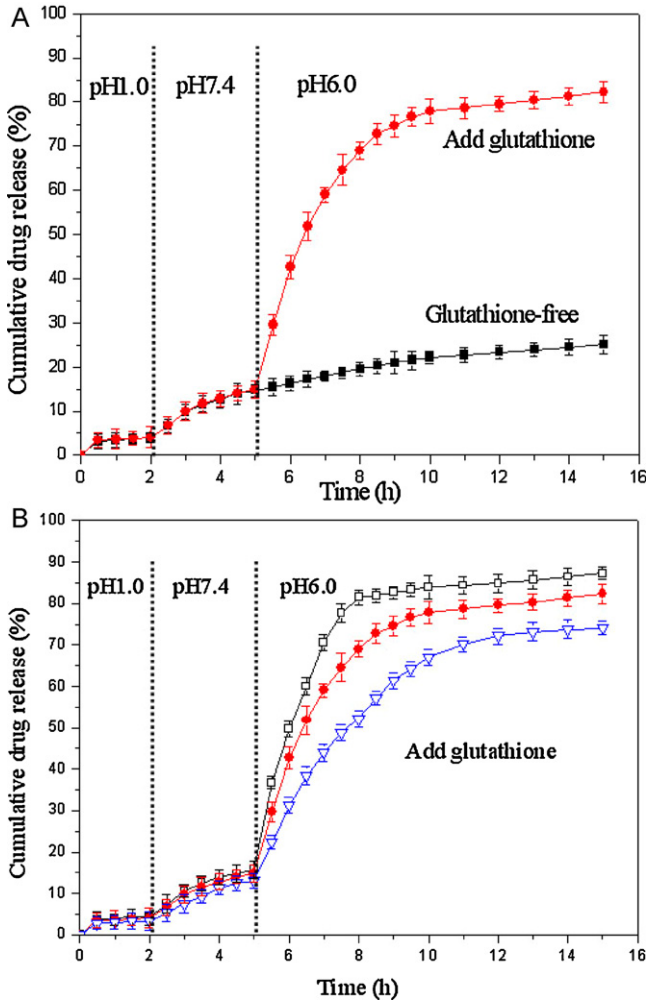

Fig. 6. (A) Release profiles of 5-ASA from NS-2: in control media (■) and in simulated gastrointestinal media (●) and (B) Release profiles of 5-ASA from NS-1 (□), NS-2 (●) and NS-3 (▽) in simulated gastrointestinal media.

the nanoparticle. The increase of pH can enhance the release of 5-ASA in hydrophilic shell but the total amount released is not too high. However, when the shell-swollen nanosphere is again placed in a reductive medium, because of the disruption of disulfide cross-linking bonds in the core, the chain relaxation leads to a rapid and nearly complete release of 5-ASA.

4. Conclusions

In this work, a novel amphiphilic 4-aminothiophenol-modified sodium alginate derivative was synthesized and its structure was characterized by FT-IR, ^{1}H NMR and UV–vis spectroscopy. In aqueous solution, TSA could self-assemble into core cross-linked nanospheres through the intra- or inter-molecular hydrophobic interactions between ATP groups and by disulfide cross-liking formed via air oxidation of free thiol groups. TEM photograph showed that the nanospheres had a spherical core–shell structure. Investigations via DLS exhibited that the nanospheres were stable and had a narrower size distribution, as well as a good pH-sensitivity. The size of nanospheres was increased upon exposure to the reductive environment. The cell viability assay suggested the nanospheres had no evident cytotoxicity. The in vitro release profiles revealed that, the cumulative amount of 5-ASA released over 15 h from the drug-loaded nanospheres in the GSH-free media was around 25%, while the release of 5-ASA was increased markedly in pH 6.0 medium with micromolar GSH. The disulfide cross-linked nanospheres may be useful in the delivery of 5-ASA to the sites of IBD, and their further investigations are in progress.

Acknowledgements

This work was financially supported by the Innovation Research Fund of Wuhan University of Technology (ZY-HG-010), and National University Student Innovation Test plan of Wuhan University of Technology (No. 091049772) and the Natural Science Foundation of China (No. 50973088).

References

Arrick, B. A., & Nathan, C. F. (1984). Glutathione metabolism as a determinant of therapeutic efficacy: A review. *Cancer Research*, *44*, 4224–4232.
Aslund, F., Berndt, K. D., & Holmgren, A. (1997). Redox potentials of glutaredoxins and other thiol-difulfide oxireductases of the thioredoxin superfamily determined by direct protein–protein redox equilibria. *Journal of Biological Chemistry*, *272*, 30780–30786.
Bernkop, S. A., Hornof, M., & Zoidl, T. (2003). Thiolated polymers-thiomers: Synthesis and in vitro evaluation of chitosan-2-iminothiolane conjugates. *International Journal of Pharmaceutics*, *260*, 229–237.
Dahan, A., Amidon, G. L., & Zimmermann, E. M. (2010). Drug targeting strategies for the treatment of inflammatory bowel disease: A mechanistic update. *Expert Review of Clinical Immunology*, *6*(4), 543–550.
Finley, J. W., Wheeler, S. C., & Witt, S. C. (1981). Oxidation of glutathione by hydrogen peroxide and other oxidizing agents. *Journal of Agriculture and Food Chemistry*, *29*, 404–407.
George, M., & Abraham, T. E. (2006). Polyionic hydrocolloids for the intestinal delivery of protein drugs: Alginate and chitosan: A review. *Journal of Controlled Release*, *114*, 1–14.
Gomez, C. G., Rinaudo, M., & Villar, M. A. (2007). Oxidation of sodium alginate and characterization of the oxidized derivatives. *Carbohydrate Polymers*, *67*, 296–304.
Hamidi, M., Azadi, A., & Rafiei, P. (2008). Hydrogel nanoparticles in drug delivery. *Advanced Drug Delivery Reviews*, *60*, 1638–1649.
Hooper, L. V., Wong, M. H., Thelin, A., Hansson, L., Falk, P. G., & Gordon, J. I. (2001). Molecular analysis of commensal host–microbial relationships in the intestine. *Science*, *291*, 881–884.
Hua, S., & Wang, A. (2009). Synthesis, characterization and swelling behavior of sodium alginate-g-poly (acrylic acid)/sodium humate superabsorbent. *Carbohydrate Polymers*, *75*, 79–84.
Lamprecht, A., Schafer, U., & Lehr, C. M. (2001). Size-dependent bioadhesion of micro- and nanoparticulate carriers to the inflamed colonic mucosa. *Pharmaceutical Research*, *18*, 788–793.
Makhlof, A., Tozuka, Y., & Takeuchi, H. (2009). pH-sensitive nanospheres for colon-specific drug delivery in experimentally induced colitis rat model. *European Journal of Pharmaceutics and Biopharmaceutics*, *72*, 1–8.
Nagpal, D., Singh, R., Gairola, N., Bodhankar, S. L., & Dhaneshwar, S. (2006). Mutual azo prodrug of 5-aminosalicylic acid for colon targeted drug delivery: Synthesis, kinetic studies and pharmacological evaluation. *Indian Journal of Pharmaceutical Sciences*, *68*, 171–178.
Nakase, H., Okazaki, K., Tabata, Y., Uose, S., Ohana, M., Uchida, K., et al. (2000). Development of an oral drug delivery system targeting immune-regulating cells in experimental inflammatory bowel disease: A new therapeutic strategy. *Journal of Pharmacology and Experimental Therapeutics*, *292*, 15–21.
Pourjavadi, A., Sadeghi, M., & Hosseinzadeh, H. (2004). Modified carrageenan 5. Preparation, swelling behavior, salt- and pH-sensitivity of partially hydrolyzed crosslinked carrageenan-graft-polymethacrylamide superabsorbent hydrogel. *Polymers for Advanced Technologies*, *15*, 645–653.
Sather, H. V., Holme, H. K., Maurstad, G., Smidsrød, O., & Stokke, B. T. (2008). Polyelectrolyte complex formation using alginate and chitosan. *Carbohydrate Polymers*, *74*, 813–821.
Sinha, V. R., & Kumria, R. (2003). Microbially triggered drug delivery to the colon. *European Journal of Pharmaceutical Science*, *18*, 3–18.
Stein, J., Ries, J., & Barret, K. E. (1998). Disruption of intestinal barrier function associated with experimental colitis: Possible role of mast cells. *American Journal of Physiology*, *274*, 203–209.
Stirrup, V., Evans, D. F., Ledingham, S., Thomas, M., Pye, G., & Hardcastle, J. D. (1990). *Proceeding of the world congress of gastroenterology, digestive endoscopy and coloproctology* Sydney.
Sundar, S., Kundu, J., & Kundu, S. C. (2011). Biopolymeric nanoparticles. *Science and Technology of Advanced Materials*, *11*, 13, 014104.
Wilding, I. R., Davis, S. S., & O'Hagan, O. T. (1994). Targeting of drugs and vaccines to the gut. *Pharmacology Therapeutics*, *62*, 97–124.
Yang, L., Chu, J. S., & Fix, J. A. (2002). Colon-specific drug delivery: New approaches and in vitro/in vivo evaluation. *International Journal of Pharmaceutics*, *235*, 1–15.
Zhao, H., & Heindel, N. D. (1991). Determination of degree of substitution of formyl groups in polyaldehyde dextran by the hydroxylamine hydrochloride method. *Pharmaceutical Research*, *8*(3), 400–402.